Contrast-enhanced T1-weighted three-dimensional gradient-echo MR imaging of the whole spine for intradural tumor dissemination.

T Sugahara, Y Korogi, T Hirai, Y Shigematu, Y Ushio and M Takahashi

AJNR Am J Neuroradiol 1998, 19 (9) 1773-1779
http://www.ajnr.org/content/19/9/1773

AJNR Am J Neuroradiol 19:1773–1779, October 1998

Contrast-Enhanced T1-Weighted Three-dimensional Gradient-Echo MR Imaging of the Whole Spine for Intradural Tumor Dissemination

Takeshi Sugahara, Yukunori Korogi, Toshinori Hirai, Yoshinori Shigematu, Yukitaka Ushio, and Mutsumasa Takahashi

BACKGROUND AND PURPOSE: **When evaluating intradural tumor dissemination in the spine, contrast-enhanced T1-weighted 2D spin-echo (2D-SE) images are frequently problematic because most of the lesions are very small. Our purpose was to compare 2D-SE images with 3D gradient-echo (3D-GE) postcontrast images to determine which technique is better for depicting intradural tumor dissemination.**

METHODS: **Ten patients with and 10 without intradural tumor dissemination were examined prospectively with MR imaging. After contrast administration, all patients underwent sagittal imaging with 2D-SE and 3D-GE sequences. Subsequently, the 2D-SE, 3D-GE, and multiplanar reconstruction (MPR) images of the 3D-GE sequence were evaluated for image quality, lesion detectability, signal-to-noise ratio (SNR), and contrast-to-noise ratio (CNR) of the disseminated lesions.**

RESULTS: **Although delineation of spinal cord from CSF was slightly poorer on the 3D-GE sequences than on the 2D-SE sequences, the difference was not significant. In the evaluation of image artifacts and contrast between spinal cord and CSF, there was no significant difference. In seven patients with nodular enhancement, the 3D-GE sequence detected 46 lesions and the 2D-SE sequence detected 36. With MPR, the greatest number of lesions (n = 51) was detected, and vascular enhancement was clearly distinguished. There was no difference in SNR and CNR of lesions between the 3D-GE and 2D-SE sequences.**

CONCLUSION: **The contrast-enhanced 3D-GE technique offers advantages over 2D-SE imaging in detecting intradural tumor dissemination, especially when the MPR technique is applied. This technique should be used for detecting intradural tumor dissemination.**

As part of the diagnostic evaluation of patients with suspected intradural tumor dissemination from malignant intracranial tumors, contrast-enhanced MR imaging of the spine and CSF cytologic examination are commonly used for determining clinical staging, prognosis, and response to treatment (1). Although the contrast-enhanced T1-weighted 2D spin-echo (2D-SE) technique is useful in the evaluation of intraaxial metastases and leptomeningeal dissemination in the head, problems may occur in the detection of tumor dissemination in the spine: examination of the whole spine is time-consuming if the axial images are acquired after the sagittal images, and normal intravascular enhancement of the medullary veins is problematic because these vessels are situated at the surface of the spinal cord and are sometimes difficult to distinguish from pathologic conditions (2, 3). The past few years have witnessed the development of a multitude of MR gradient-echo (GE) sequences. However, their utility, to our knowledge, has not been studied systematically. Therefore, we compared the 2D-SE technique with the 3D-GE technique after contrast injection to determine which sequence was better for detecting intradural tumor dissemination.

Received February 5, 1998; accepted after revision July 6.

From the Departments of Radiology (T.S., Y.K., T.H., Y.S., M.T.) and Neurosurgery (Y.U.), Kumamoto University School of Medicine, 1–1–1 Honjo, Kumamoto 860, Japan.

Address reprint requests to Takeshi Sugahara, MD, Department of Radiology, Kumamoto University School of Medicine, 1–1–1 Honjo, Kumamoto 860–0811, Japan.

Methods

Subjects

Contrast-enhanced MR imaging of the spine was performed prospectively in 10 patients with and in 10 without intradural

tumor dissemination. The 10 patients with intradural tumor dissemination included five males and five females (mean age, 46 years; range, 3 to 66 years) with medulloblastoma (n = 2), germinoma (n = 2), malignant ependymoma (n = 2), glioblastoma (n = 1), anaplastic astrocytoma (n = 1), pilocytic astrocytoma (n = 1), and lung carcinoma (n = 1).

In one patient with malignant ependymoma, the presence of tumor dissemination in the spine was confirmed by autopsy. One patient with cerebellar pilocytic astrocytoma had no local recurrence for 12 years after surgical resection. However, MR examination, performed when the patient reported neurologic symptoms, disclosed intraspinal tumors. Since dissemination from pilocytic astrocytoma is rare and 12 years had passed since surgery, surgical resection was performed to confirm the histopathologic findings. In one patient with glioblastoma, partial tumor resection in the spine was performed because intraspinal tumors occupying the canal space caused neurologic deterioration. In one patient with germinoma, which was diffusely disseminated in both intracranial and intraspinal subarachnoid spaces, open biopsy of the intraspinal lesion was performed to obtain histologic proof of diagnosis. In the remaining six patients, final diagnosis was based on findings at follow-up MR imaging, which disclosed that the enhanced lesions either had disappeared after radiochemotherapy or had progressively increased. All 10 patients had follow-up MR imaging 9 months or more (maximum, 22 months) after the initial MR study.

The other 10 patients (five males and five females; mean age, 28 years; range, 10 to 63 years), who served as control subjects, underwent contrast-enhanced MR imaging of the spine because of clinical signs of multiple sclerosis (n = 6) as part of a routine examination to rule out canal stenosis caused by spondylosis (n = 2) or to rule out tumor after clinical diagnosis of myelopathy (n = 2).

MR Imaging

MR imaging was performed at 1.5 T with a circular polar phased-array spinal coil, which facilitates imaging along the full length of the spine. To reduce the examination time, the entire spine was imaged during one session. After the sagittal T1-weighted SE and T2-weighted fast SE imaging sequences were obtained, sagittal contrast-enhanced 3D-GE and 2D-SE imaging was performed. All sagittal images were acquired with a rectangular field of view (FOV) to obtain finer spatial resolution in the phase-encoding direction. The 10 patients with intradural tumor dissemination underwent 2D-SE and 3D-GE studies after administration of 0.15 mmol/kg of contrast material; the 10 without intradural tumor dissemination were examined after administration of 0.10 mmol/kg of contrast material. The T1-weighted SE and contrast-enhanced 2D-SE sequences in the sagittal plane were acquired with parameters of 500/15/1 (TR/TE/excitations), 4-mm-thick sections, and a 0.4-mm intersection gap. The acquisition time was 4 minutes 19 seconds. The T2-weighted fast SE sequence in the sagittal plane was performed with parameters of 4000/120/2 (TR/TE_{eff}/excitations), 4-mm-thick sections, and a 0.4-mm intersection gap. The acquisition time was 4 minutes 52 seconds. The parameters for the contrast-enhanced 3D-GE sequence were 35/6/1 (TR/TE/excitations), 1-mm-thick sections, and a flip angle of 35°. The acquisition time was 6 minutes 34 seconds. For all sequences, a 32- to 48-cm FOV and a 256 × 512 matrix were used. The contrast-enhanced 3D-GE images were reconstructed with a multiplanar reconstruction (MPR) technique, yielding images in all three orthogonal planes. The total scan time ranged from 25 to 40 minutes.

Image Analysis

As previously reported (3), enhancement was attributed to spinal cord vessels on the basis of typical location of the vessels and whether the enhancement was linear, uniform in size, and continuous in the craniocaudal direction on sagittal images. Enhancement was attributed to vessels on the surface of the nerve roots when it was found adjacent to the nerve root and was uniform in size. Enhancement was attributed to intradural-extramedullary tumor deposits when it appeared nodular, lacked craniocaudal contiguity, and was nonuniform in size.

Qualitative Analysis

Two radiologists, who were blinded to the clinical histories of all 20 patients, independently evaluated the image quality and artifacts on the sagittal contrast-enhanced 2D-SE and 3D-GE images for the following: contrast between spinal cord and CSF, delineation of spinal cord from CSF, motion artifacts, and artifacts induced by pulsation transmitted from the heart and large vessels. Judgments regarding contrast and delineation of spinal cord from CSF were ranked on a four-point scale, as follows: 1 = poor, 2 = fair, 3 = good, and 4 = excellent. Responses regarding artifacts were ranked similarly as 1 = absent, 2 = mild, 3 = moderate, and 4 = severe.

The radiologists then evaluated the appearance of the lesions on the sagittal contrast-enhanced 2D-SE, 3D-GE, and MPR images. The MPR images were always analyzed in conjunction with the corresponding sagittal contrast-enhanced 3D-GE images because of the potential for misinterpretation inherent in the evaluation of MPR images alone. On a set of MR images, disseminated lesions were coded as present, absent, or questionable. The final interpretation was obtained by consensus.

Quantitative Analysis

The signal-to-noise ratio (SNR) and contrast-to-noise ratio (CNR) on the images of patients with intradural tumor dissemination were calculated by one radiologist, who used the following formulas: SNR = SI lesion/noise, and CNR = (SI lesion − SI cord)/noise, where SI indicates signal intensity and noise indicates SD of noise along the phase-encoding direction in spaces outside the body. The SI was measured by using an electric cursor that encompassed a large portion of the lesion, and the same cursor size was used to measure the SI of the adjacent CSF and noise outside the patient. For patients who had more than five lesions in any one of the cervical, thoracolumbar, and cauda equina segments, five lesions were chosen at random for evaluation. To minimize the partial volume effect on CNR measurements, the larger lesions were chosen. When the enhanced lesions were small, the image was magnified on the monitor and regions of interest were placed.

Statistical Analysis

The statistical significance of the quantitative and qualitative results was determined by using Student's *t*-test. Interobserver agreement for the independent analysis of lesion detection (before the final interpretation by consensus) was assessed with the κ statistic (4). The difference was considered statistically significant when the *P* value was less than .01.

Results

Qualitative Analysis

Image Quality.—The results of the qualitative evaluation of the images and artifacts are summarized in Table 1. The contrast and the delineation of spinal cord from CSF were poorer on the contrast-enhanced 3D-GE sequence than on the contrast-enhanced SE sequence ($P = .011$ and $P < .001$, respectively), although the contrast-enhanced 3D-GE sequence was of satisfactory quality. The artifacts induced by patient motion and pulsation of the heart and large

TABLE 1: Results of qualitative evaluation of image quality and artifacts for contrast-enhanced 2D-SE versus 3D-GE sequences in 20 patients

Parameter	2D-SE	3D-GE
Contrast between cord and CSF	3.40 ± 0.49	3.00 ± 0.45
Delineation of cord from CSF	3.45 ± 0.50	2.95 ± 0.59*
Motion artifacts	1.20 ± 0.51	1.10 ± 0.30
Flow artifacts	1.50 ± 0.50	1.50 ± 0.50

Note.—Data indicate mean ± SD; 2D-SE, T1-weighted 2D spin-echo; 3D-GE, T1-weighted 3D gradient-echo.

* $P < .01$.

TABLE 2: Results of lesion detectability on contrast-enhanced 2D-SE versus 3D-GE sequences in 10 patients with intradural tumor dissemination

Imaging Sequence	Disseminated Lesions	
	Questionable	Present
2D-SE	7	36
3D-GE	4	46
3D-GE + MPR	0	51

Note.—Data indicate mean ± SD; 2D-SE, T1-weighted 2D spin-echo; 3D-GE, T1-weighted 3D gradient-echo; MPR, multiplanar reconstruction images.

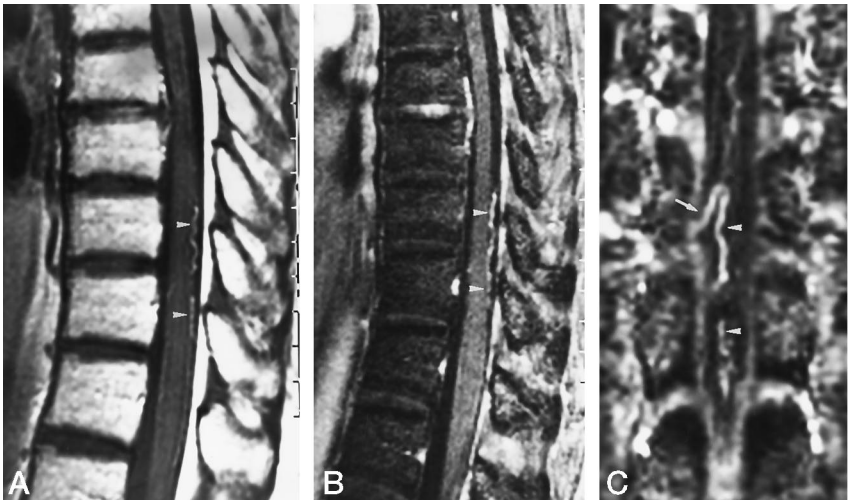

FIG 1. 12-year-old girl (control patient).

A and *B*, Linear enhancement on the surface of the spinal cord is seen on sagittal image obtained with the contrast-enhanced 2D-SE technique (*arrowheads, A*) and on sagittal image obtained with the contrast-enhanced 3D-GE technique (*arrowheads, B*).

C, The coronal image, reconstructed from the contrast-enhanced 3D-GE image, clearly shows continuous linear enhancement related to the median vein (*arrowheads*). The medullary vein (*arrow*) was identified by the continuity to the median vein on the serial MR images.

vessels were not different between the contrast-enhanced 2D-SE sequence and the 3D-GE sequence.

Lesion Detectability.—In the two patients with malignant ependymoma and the one with germinoma, which were proved by open biopsy or autopsy, tumor dissemination was diffusely continuous through the intradural space and could be identified on both the contrast-enhanced 2D-SE and 3D-GE images. These three patients were excluded from the evaluation of lesion detectability because the number of diffusely continuous tumor deposits could not be counted. In the remaining seven patients with intradural tumor dissemination, the number of tumor deposits was counted by two other observers. Enhancement that was linear, uniform in size, and continuous was interpreted as spinal cord vessels (Fig 1) or vessels on the surface of the nerve roots.

Table 2 summarizes the results of lesion detection in the patients with intradural tumor dissemination, excluding the three patients with diffusely continuous intradural tumor dissemination. Thirty-six lesions ranked as present on the contrast-enhanced 2D-SE images were also interpreted as present on the contrast-enhanced 3D-GE images. Four of eight lesions were ranked as absent and four of seven lesions as questionable on the contrast-enhanced 2D-SE images but interpreted as present on the contrast-enhanced 3D-GE images. The remaining seven lesions were interpreted as questionable on the contrast-enhanced 3D-GE images. However, these lesions were clearly depicted on the MPR images and ranked as present (Fig 2). One of two lesions disseminated on the lateral surface of the spinal cord could not be detected on the contrast-enhanced 2D-SE and 3D-GE images. With use of the MPR technique, this lesion was clearly demonstrated (Fig 3). Diffusely continuous intradural tumor dissemination was seen in three patients, and lesion extension was depicted comparably on the contrast-enhanced 2D-SE and 3D-GE images. There was good interobserver agreement for the assessment of lesion detection ($\kappa = .87$, $P < .01$).

In one patient with tumor dissemination from cerebellar pilocytic glioma, MR imaging was performed to investigate whether intradural tumor dissemination was present. A minimally enhanced lesion was observed in the thoracic canal but was not clearly depicted on the contrast-enhanced 2D-SE images. This lesion was interpreted as questionable. However, the contrast-enhanced 3D-GE images clearly depicted the enhanced lesion and, therefore, this patient underwent resection of the enhanced lesion, which was confirmed as intradural tumor dissemination (Fig 4).

In three patients without intradural tumor dissemination, two lesions in two patients were ranked as questionable on both contrast-enhanced 2D-SE and 3D-GE images, and one lesion in one patient was ranked as questionable on the contrast-enhanced 2D-SE image and as absent on the contrast-enhanced 3D-GE image because the spotty enhancements were observed on only one sagittal or parasagittal section

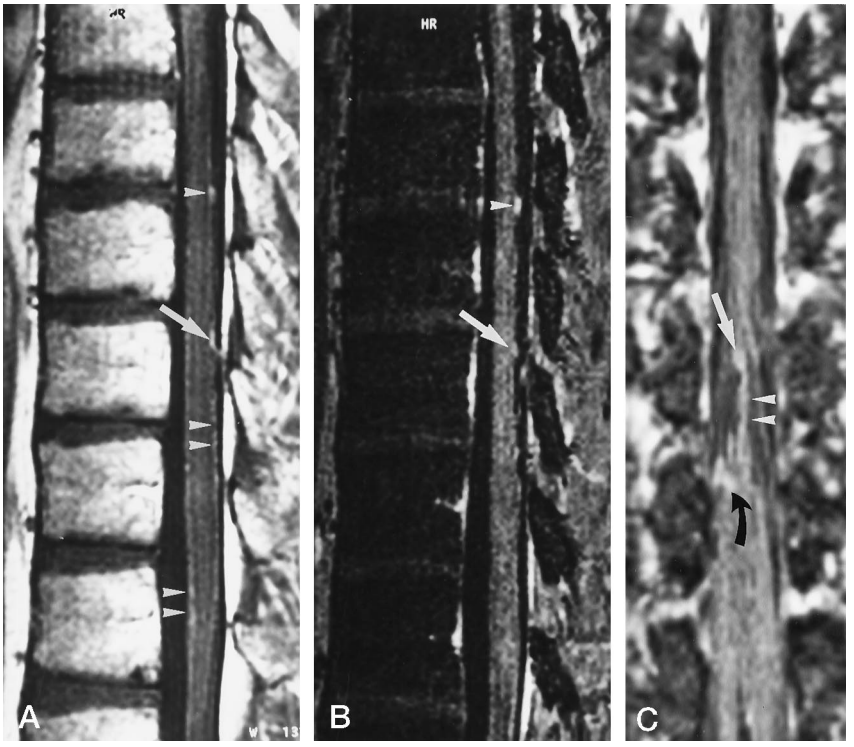

FIG 2. 8-year-old girl with tumor dissemination from cerebellar medulloblastoma. The final diagnosis was based on follow-up MR studies in which all enhanced lesions completely disappeared after radiochemotherapy.

A, On sagittal contrast-enhanced 2D-SE image, two areas of linear enhancement were observed on the surface of the spinal cord (*arrow, arrowheads*). These areas were ranked as questionable because they could not be differentiated from a tortuous posterior median vein. The areas of linear enhancement along the ventral and dorsal cord surfaces were consistent with the anterior and posterior median veins, respectively.

B, On sagittal contrast-enhanced 3D-GE image, one lesion was ranked as present because of nodular and discontinuous enhancement (*arrowhead*). However, another lesion (*arrow*) was interpreted as questionable because the area of enhancement was relatively small and the interpreters concluded that the enhancement could not be differentiated from a tortuous posterior median vein.

C, On coronal image, reconstructed from the contrast-enhanced 3D-GE image, the enhanced lesion, which was ranked as questionable on the contrast-enhanced 3D-GE image, is clearly seen and ranked as present (*straight arrow*). Another tumor dissemination, which cannot be detected on the sagittal MR images, is observed (*curved arrow*). The typical linear enhancement of the posterior median vein (*arrowheads*) is often observed on coronal MPR images.

and thus the interpreters could not determine whether to attribute the enhancement to normal veins or to tumor deposits. However, with the use of the MPR technique, these lesions were confirmed as normal vascular enhancement, such as seen for the median or great medullary veins, because enhancement was continuous and uniform in size and vessels were typically located.

Quantitative Analysis

The results of the quantitative evaluation are summarized in Table 3. The SNR and CNR for the contrast-enhanced 2D-SE sequence did not differ significantly from those for the 3D-GE sequence. The SNR for the contrast-enhanced 3D-GE sequence was slightly lower but the CNR was higher than for the contrast-enhanced 2D-SE images.

Discussion

A correct diagnosis of intradural tumor dissemination is essential for patients with malignant CNS tumor, especially germinoma, medulloblastoma, and malignant glioma, because of the implications for treatment planning and prognosis. The reported frequency of intradural tumor dissemination in germinoma is 52% to 60% as detected with cytologic examination (5, 6), and those reports recommend irradiation of the cerebrospinal axis at 20 to 24 Gy to improve survival rate. In medulloblastoma, the reported frequency of intradural tumor dissemination is 17% to 46% (7–9), with patients in whom spinal cord involvement is apparent at the time of diagnosis most at risk for recurrence in the spinal cord. The frequency of intradural tumor dissemination has been reported at 33% in children with malignant gliomas, and contrast-enhanced T1-weighted MR imaging was recommended for postoperative evaluation of the spinal axis because one of the risk factors for intradural tumor dissemination is the operation itself, and the mortality rate is very high once intradural tumor dissemination has occurred (10). In another study of intradural tumor dissemination from malignant tumors, a prompt diagnosis was concluded to be essential to preserve normal neural function, local tumor control, and spinal stability (11). To determine whether intradural tumor dissemination is present, CSF cytologic examinations are frequently performed, but these techniques are inherently invasive and have the risk of sampling error (12).

Despite the advantages of phased-array coils and 3D imaging, it has not been demonstrated that these techniques have the potential to reliably depict the abnormal contrast enhancement of intradural diseases in the spine, especially in patients with intradural tumor dissemination who should undergo whole spine examination for treatment planning. Therefore, we evaluated the depiction of intradural tumor dissemination as well as the normal appearance of the whole spine and the image quality achieved with the contrast-enhanced 3D-GE technique using the circular polar phased-array coil to determine whether this technique is a potential alternative to the contrast-enhanced 2D-SE technique.

We found that the contrast-enhanced 2D-SE im-

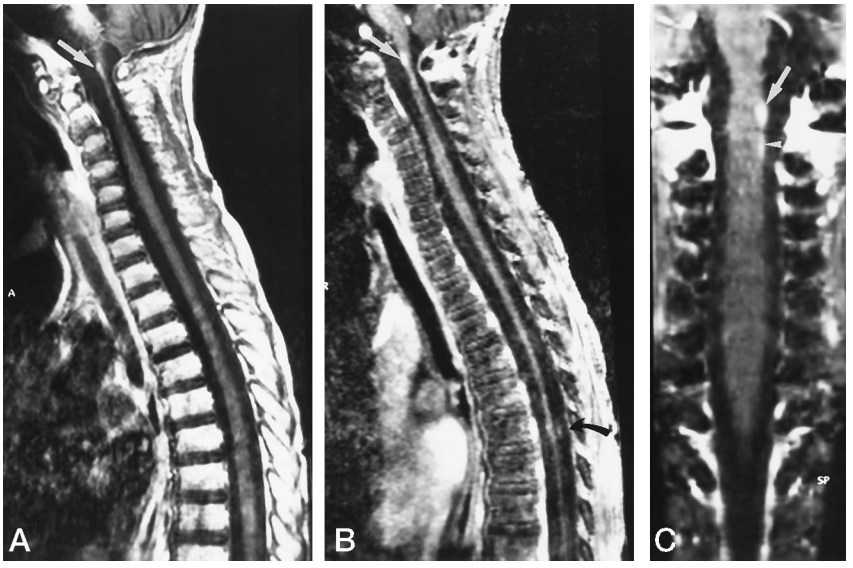

FIG 3. 3-year-old boy with tumor dissemination from cerebellar medulloblastoma. The final diagnosis was based on follow-up MR studies in which all enhanced lesions completely disappeared after radiochemotherapy.

A–C, Minimal enhancement (*straight arrows*) is observed on the surface of the spinal cord on the sagittal contrast-enhanced 2D-SE image (*A*) and on the 3D-GE image (*B*). This enhancement was ranked as present on both images. The coronal image (*C*), reconstructed from the contrast-enhanced 3D-GE image, shows two areas of nodular enhancement, one of which (*arrowhead*) was not detected on either the sagittal contrast-enhanced 2D-SE image or the 3D-GE image. In this case, image artifacts are more conspicuous on the 3D-GE image than on the 2D-SE image, and some of the artifacts resemble tumor dissemination (*curved arrow, B*). However, motion artifacts can be easily distinguished from intradural tumor dissemination because the signal intensity of artifacts is lower than that of tumor dissemination, the origin of motion artifacts is easily identified, and the relationship between the artifacts and the spinal cord is clear.

ages in the sagittal plane frequently failed to depict intradural tumor dissemination. These images were acquired by using 4-mm-thick sections and a 0.4-mm intersection gap to minimize the reduction in SNR and T1 contrast (13–15). With these parameters, the voxel sizes for the contrast-enhanced 2D-SE images ranged from 1.56 to 3.52 mm^3, whereas those for the 3D-GE images ranged from 0.39 to 0.88 mm^3. Voxel volume is inversely proportional to spatial resolution, which was 400% greater for the contrast-enhanced 3D-GE images than for the 2D-SE images. In addition to providing markedly reduced voxel volumes, the use of contrast-enhanced 3D-GE imaging also results in the elimination of intersection gaps. Intradural tumor dissemination is minimal in some patients and can be situated anywhere in the spine. Therefore, the imaging technique must provide high spatial resolution and cover the entire spine.

The contrast-enhanced 3D-GE technique also provided SNR and CNR of intradural tumor dissemination comparable to that available with the contrast-enhanced 2D-SE technique. As indicated in a previous report on intracranial lesions (16), the SNR of 3D-GE images is inherently lower than that of SE images because the voxel volumes are very small and the SNR on the 3D-GE images is affected by cross-excitation between adjacent imaging sections and by such effects as artifacts due to motion, susceptibility, and chemical shift. In addition, SNR is influenced by variable parameters such as TR, TE, flip angle, and number of partitions (17, 18). However, the SNR and CNR of disseminated lesions on 3D-GE images are equivalent to those on 2D-SE images. Those results may have been caused by the short TE of 6 milliseconds used for the 3D-GE sequence, which minimized signal loss from the T2 decay effect, and by the flip angle of 35°, which enhanced the T1 effects (19). The thin sections used for the 3D-GE sequence also may have minimized signal loss from the partial volume effects.

The excitation of a large volume of tissue rather than individual sections leads to another important advantage of the contrast-enhanced 3D-GE technique. Contrast-enhanced 3D-GE images can be reformatted in any orthogonal or oblique imaging plane after the images have been acquired and the patient has left the department. Such reformations may also be acquired along a tilted or curved plane and can be generated in near real time by using current image-processing workstations. Although the plane is varied according to the suspected location of the abnormality, the lesions located at the lateral surface of the spinal cord are not readily depicted by the contrast-enhanced 2D-SE technique and, if disseminated lesions are overlooked on the initial 2D-SE images in the sagittal plane, another plane may not be scanned. It is possible to scan the entire spine in the coronal or axial plane, but this is so time-consuming that it is clinically impractical.

Depiction of the median spinal and great medullary veins on coronal images reformatted from 3D-GE images is often advantageous. It may be difficult to ascertain whether these vascular structures are pathologic lesions or not. In the thoracolumbar spine, the anterior median vein is usually a single, midline trunk, ranging in size from 0.5 to 1.5 mm (20). The posterior median vein and other posterior coronal veins tend to be more tortuous than the veins on the anterior and lateral cord surfaces, and their tortuosity increases with age (21). The medullary veins are not present at every segmental level and the number of anterior medullary veins ranges from eight to approximately 20 (18, 20). The largest (1.5 to 2.0 mm) are in the thoracolumbar region, identified as the great anterior and/or posterior medullary veins (22). Although one previous report indicated that these veins are differ-

FIG 4. A 20-year-old man with dissemination from pilocytic astrocytoma. The final diagnosis was based on surgical findings.

A, On the parasagittal contrast-enhanced 2D-SE image, minimal enhancement is seen on the surface of the spinal cord (*arrow*). This enhancement was ranked as questionable.

B, Nodular enhancement (*arrow*) is clearly depicted on the parasagittal contrast-enhanced 3D-GE image.

C, The coronal image, reconstructed from the contrast-enhanced 3D-GE image, clearly shows nodular enhancement related to the dissemination (*arrow*). The midline linear enhancement (*arrowheads*) below the nodular enhancement shows median vein.

TABLE 3: SNR and CNR for disseminated lesions for contrast-enhanced 2D-SE and 3D-GE sequences

Parameter	2D-SE	3D-GE
SNR	99.0 ± 71.8	71.8 ± 42.2
CNR	38.4 ± 40.4	40.4 ± 34.5

Note.—Data indicate mean ± SD; SNR, signal-to-noise ratio; CNR, contrast-to-noise ratio; 2D-SE, T1-weighted 2D spin-echo; 3D-GE, T1-weighted 3D gradient-echo.

entiated from pathologic conditions on the basis of their typical location, size, and contiguity on contrast-enhanced sagittal and axial SE images (17), differentiating between them is not necessarily easy. On the other hand, the contrast-enhanced 3D-GE sequence with the use of the MPR technique clearly depicts the continuous vascular structures and confirms the absence of tumor dissemination.

Generally, flow artifacts are accentuated on 2D-SE images after administration of contrast material owing to the intraluminal T1-shortening effects of the contrast agent (23). Gradient-moment nulling (flow compensation) techniques may reduce flow artifacts but cannot be implemented with short-TE SE imaging. The shorter TEs available with 3D-GE imaging, as well as the reduced section thickness, lead to a further reduction of flow artifacts. In contrast, patient motion during image acquisition leads to more severe artifacts on the 3D-GE images than on the 2D-SE images, because phase encoding is performed in two axes rather than one. Such artifacts may result in image blurring or in superimposition of anatomic structures, either of which obscures anatomic detail (17). In this study, the motion artifacts were not different for the two sequences, perhaps because with the contrast-enhanced 3D-GE sequence not only is the imaging time relatively short but also the flow and pulsation artifacts are reduced. Although the 3D-GE images may produce more severe motion artifacts than the 2D-SE images owing to the longer acquisition time, those artifacts can be easily distinguished from tumor dissemination by carefully observing their signal intensity, origin, and relationship to the spinal cord.

In this study, 10 patients with and 10 without intradural tumor dissemination underwent contrast-enhanced 2D-SE and 3D-GE studies after administration of 0.15 and 0.10 mmol/kg of contrast material, respectively. Because previous studies in the brain have shown potential benefits from the use of 0.2 to 0.3 mmol/kg of contrast material, similar benefits may be found with use of higher doses in the spine (24, 25). However, another study (19) showed that a triple dose did not result in detection of intradural tumor dissemination in the spine of children; and, at present, an optimal dose has not been determined. On the basis of the facts stated above and from an economic standpoint, we used a dose of 0.15 mmol/kg for patients in whom intradural tumor dissemination was suspected and a dose of 0.10 mmol/kg for those in whom such dissemination was not suspected.

Conclusion

Contrast-enhanced 3D-GE imaging of the whole spine offers important advantages over contrast-enhanced 2D-SE imaging. Tumor dissemination in the spine is detected better on contrast-enhanced 3D-GE images than on contrast-enhanced 2D-SE images. Therefore, we recommend the routine use of contrast-enhanced 3D-GE imaging for evaluation of tumor dissemination in the spine.

References

1. Wolden SL, Wara WM, Larson DA, et al. **Radiation therapy for primary intracranial germ-cell tumors.** *Int J Radiat Oncol Biol Phys* 1995;32:943–949
2. Lane JI, Koeller KK, Atkinson JL. **Contrast-enhanced radicular veins on MR of the lumbar spine in an asymptomatic study group.** *AJNR Am J Neuroradiol* 1995;16:269–273
3. Tam JK, Bradley WG, Goergen SK, et al. **Patterns of contrast enhancement in the pediatric spine at MR imaging with single- and triple-dose gadolinium.** *Radiology* 1996;198:273–278
4. Cohen J. **A coefficient of agreement for nominal scales.** *Educ Psychol Meas* 1960;20:37–46
5. Shibamoto Y, Oda Y, Yamashita J, Takahashi M, Kikuchi H, Abe M. **The role of cerebrospinal fluid cytology in radiotherapy planning for intracranial germinoma.** *Int J Radiat Oncol Biol Phys* 1994;29:1089–1094
6. Sano K. **Pinealoma in children.** *Childs Brain* 1976:2;67–72
7. Deutsch M. **Medulloblastoma: staging and treatment outcome.** *Int J Radiat Oncol Biol Phys* 1988;14:1103–1107
8. Allen JC, Epstein F. **Medulloblastoma and other primary malignant neuroectodermal tumors of the CNS: the effect of patients' age and extent of disease on prognosis.** *J Neurosurg* 1982;57:446–451
9. Berry MP, Jenkin RDT, Keen CW, et al. **Radiation treatment for medulloblastoma: a 21-year review.** *J Neurosurg* 1981;55:43–51
10. Grabb PA, Albright AL, Pang D. **Dissemination of supratentorial malignant gliomas via the cerebrospinal fluid in children.** *Neurosurgery* 1992;30:64–71
11. Delaney TS, Oldfield EH. **Spinal cord compression.** In: DeVita VT, Hellman S, Rosenberg SA, eds. *Cancer.* 4th ed. Philadelphia: Lippincott; 1993:2118–2126
12. Little JR, Dale AJD, Okazaki H. **Meningeal carcinomatosis: clinical manifestation.** *Arch Neurol* 1974;30:138–143
13. Bradley WG, Glenn BJ. **The effect of variation in slice thickness and interslice gap on MR lesion detection.** *AJNR Am J Neuroradiol* 1987;8:1057–1062
14. Kucharczyk W, Crawley AP, Kelly WM, Henkelman RM. **Effect of multislice interference on image contrast in T2- and T1-weighted MR images.** *AJNR Am J Neuroradiol* 1988;9:443–451
15. Schwaighofer BW, Yu KK, Mattrey RF. **Diagnostic significance of interslice gap and imaging volume in body MR imaging.** *AJR Am J Roentgenol* 1989;153:629–632
16. Mirowitz SA. **Intracranial lesion enhancement with gadolinium: T1-weighted spin-echo versus three-dimensional Fourier transform gradient-echo MR imaging.** *Radiology* 1992;185:529–534
17. Carlson J, Crooks L, Ortendahl D, Kramer DM, Kaufman L. **Signal-to-noise ratio and section thickness in two-dimensional versus three-dimensional Fourier transform MR imaging.** *Radiology* 1988;166:266–270
18. Lasjaunias P, Berenstein A. **Functional vascular anatomy of the brain, spinal cord and spine. In: Lasjaunias P, Berestein P, eds.** *Surgical Neuroangiography.* New York: Springer; 1987;3:15–87
19. Tam JK, Bradley WG, Goergen SK, et al. **Patterns of contrast enhancement in the pediatric spine at MR imaging with single- and triple-dose gadolinium.** *Radiology* 1996;198:273–278
20. Runge VM, Kirsch JE, Thomas GS, Mugler JP III. **Clinical comparison of three-dimensional MP-RAGE and FLASH techniques for MR imaging of the head.** *J Magn Reson Imaging* 1991;1:493–500
21. Gillilan LA. **Veins of the spinal cord: anatomic details: suggested clinical applications.** *Neurology* 1970;20:860–868
22. Tam JK, Bradley WG Jr, Goergen SK, et al. **Patterns of contrast enhancement in the pediatric spine at MR imaging with single- and triple-dose gadolinium.** *Radiology* 1996;198:273–278
23. Richardson DN, Elster AD, Williams DW III. **Gd-DTPA-enhanced MR images: accentuation of vascular pulsation artifacts and correction by using gradient-moment nulling (MAST).** *AJNR Am J Neuroradiol* 1990;11:209–210
24. Yuh WT, Engleken JD, Muhonen MG, Mayr NA, Fisher DJ, Ehrhardt JC. **Experience with high dose gadolinium MR imaging in the evaluation of brain metastases.** *AJNR Am J Neuroradiol* 1992;13:335–345
25. Haustein J, Landiado M, Niendorff H, et al. **Triple-dose versus standard-dose gadopentetate dimeglumine: a randomized study in 199 patients.** *Radiology* 1993;186:855–860

Please see the Editorial on page 1595 in this issue.